

The Surface Brightness and Colour-Magnitude Relations for Fornax Cluster Galaxies

A. M. Karick¹, M. J. Drinkwater² and M. D. Gregg^{3,4}

¹*School of Physics, University of Melbourne, Victoria 3010, Australia*

²*Department of Physics, University of Queensland, Queensland 4027, Australia*

³*Department of Physics, University of California, Davis, CA 95616, USA*

⁴*Institute for Geophysics and Planetary Physics, Lawrence Livermore National Laboratory, L-413, Livermore, CA 94550, USA*

Draft version 1.0, July 14th 2002

ABSTRACT

We present BVI photometry of 190 galaxies in the central $4^\circ \times 3^\circ$ region of the Fornax Cluster observed with the Michigan Curtis Schmidt Telescope. Results from the Fornax Cluster Spectroscopic Survey (FCSS) and the Flair-II Fornax Surveys have been used to confirm the membership status of galaxies in the Fornax Cluster catalogue, FCC (Ferguson 1989). In our catalogue of 213 member galaxies, 92 (43%) have confirmed radial velocities.

In this paper we investigate the surface brightness-magnitude relation for Fornax Cluster galaxies. Particular attention is given to the sample of cluster dwarfs and the newly discovered ultra-compact dwarf galaxies (UCDs) from the FCSS (Drinkwater et al. 2000; Deady et al. 2002). We examine the reliability of the surface brightness-magnitude relation as a method for determining cluster membership and find that at surface brightnesses fainter than $22 \text{ mag arcsec}^{-2}$, it fails in its ability to distinguish between cluster members and hardly resolved background galaxies. Cluster members exhibit a strong surface brightness-magnitude relation. Both elliptical (E) galaxies and dwarf elliptical (dE) galaxies increase in surface brightness as luminosity decreases. The UCDs lie off the locus of the relation.

B-V and V-I colours are determined for a sample of 113 cluster galaxies and the colour-magnitude relation is explored for each morphological type. The UCDs lie off the locus of the colour-magnitude relation. Their mean V-I colours (~ 1.09) are similar to those of globular clusters associated with NGC 1399. The location of the UCDs on both surface brightness and colour-magnitude plots supports the “galaxy threshing” model for infalling nucleated dwarf elliptical (dE,N) galaxies (Bekki et al. 2001).

Key words: galaxies: clusters: individual: Fornax - galaxies: dwarfs - galaxies: photometry - methods: observational

1 INTRODUCTION

In recent years the relationship between ‘dwarf’ galaxies and ‘normal’ elliptical galaxies has been described as a ‘dichotomy’ - a description based on the observation that each population exhibits a unique surface brightness-luminosity relation (Ferguson & Binggeli 1994). In addition, surface brightness profiles differ between both populations. Typical profiles for elliptical (E) galaxies follow a $r^{-1/4}$ power law whereas dwarf elliptical (dE) galaxies generally follow an exponential law. Despite a lack of physical understanding, the surface brightness-magnitude relation provides one of the most fundamental means of galaxy classification and structure determination.

Over the last few decades studies of galaxy clusters have

been dominated by wide-field photographic imaging. Population studies of the Fornax Cluster (Bothun et al. 1991; Phillipps et al. 1987; Ferguson & Sandage 1988; Ferguson 1989) have traditionally combined image morphology and surface brightness measurements to provide a statistical treatment of cluster membership. By virtue of their low surface brightnesses, dwarf galaxies were traditionally classified as cluster members whereas faint galaxies with high surface brightness were assigned a background status.

Although studies of this nature have led to our present understanding of cluster populations it seems that these traditional classification techniques are not as robust as initially thought. Without known radial velocities, compact elliptical galaxies such as M32, are virtually indistin-

guishable from intrinsically luminous background E galaxies (Sandage & Binggeli 1984). The discovery of the large, low surface brightness spiral Malin 1 (Bothun et al. 1987) exemplifies the problem of membership assignment on the basis of surface brightness. This large background giant was previously classified as a foreground cluster dwarf.

Simulations of galaxy evolution based on Cold-Dark-Matter (CDM) models predict numbers of dwarf galaxies that far exceed those observed locally (Ferguson & Binggeli 1994). These models suggest that many of these low surface brightness galaxies may be missing from magnitude-limited surveys. Consequently our current understanding of the cluster luminosity function may be significantly biased towards the high-luminosity limit.

The nearby Fornax Cluster is one of the most well studied galaxy clusters. Its environment and proximity provides a rich playing field for galaxy studies over a large range of morphological types. Covering an area of nearly 40 deg^2 , Ferguson's optical catalogue of the Fornax Cluster (FCC) (Ferguson 1989) contains 2678 galaxies of which 340 are classified as "likely cluster members". Members were originally identified visually from large-scale photographic plates, primarily on the basis of morphology and surface brightness. Of the 340 "likely members", 186 were classified as dwarf galaxies and only 68 galaxies had known radial velocities.

Recently a spectroscopic survey of the Fornax Cluster (Drinkwater et al. 2000) revealed a small sample of ultra-compact dwarf galaxies (UCDs) with radial velocities indicating cluster membership. In previous studies using photographic plates, these unresolved high luminosity objects were mis-classified as foreground stars.

In this paper we present BVI photometry of 190 Fornax Cluster members obtained with the CTIO Curtis Schmidt Telescope. After constructing a $4^\circ \times 3^\circ$ mosaic of the cluster we have measured the magnitudes and surface-brightnesses of all cluster galaxies within the field. As a result we have produced a surface brightness-magnitude relation that includes a much larger range of galaxy luminosities and morphological types than has previously been achieved. Since we have a large number of galaxies with confirmed redshifts we have also investigated the use of the surface brightness-magnitude relation for cluster membership classification. Of particular interest is the high luminosity, high surface brightness extension of the dwarf population relative to the normal ellipticals and the location of the recently discovered ultra-compact dwarf galaxies.

From the surface brightness-magnitude relation the relative positions of the ultra-compact dwarfs to the remaining cluster population has enabled us to further explore their origin. Our results support analysis by Phillipps et al. (2001); Drinkwater et al. (1999); Hilker et al. (2001) and others, that the UCDs are a unique type of dwarf galaxy, possibly remnant nuclei of infalling dwarfs which have been tidally stripped through their interaction with the central cD galaxy, NGC 1399 (Bekki et al. 2001).

We have also determined the colours (B-V & V-I) of the cluster galaxies to investigate correlations with other photometric parameters and identify a possible environmental influence on cluster galaxy evolution.

In Section 2 we introduce our revised catalogue of Fornax Cluster members in the central $4^\circ \times 3^\circ$ region. Section 3 details our observations and Section 4 the photometry of

cluster members. We then discuss the surface brightness-magnitude relations for cluster members and non-members in Section 5 and galaxy colours in Section 6. We conclude with a discussion and summary of our results in Sections 7 and 8.

2 CLUSTER GALAXIES

Our sample of Fornax Cluster galaxies is largely based on Ferguson's optical *Fornax Cluster Catalogue (FCC)* of 340 members. The 205 member galaxies from the FCC which lie in the central $4^\circ \times 3^\circ$ region of the cluster form the basis of our sample. In the original FCC only 52 (25%) galaxies in the mosaic region were confirmed by their radial velocities as cluster members. We have incorporated the results from a number of recent spectroscopic surveys of the cluster (Drinkwater et al. 1999; Hilker et al. 1999; Drinkwater et al. 2001), in which membership classifications have been reassigned. Our final catalogue for the central $4^\circ \times 3^\circ$ region contains 213 cluster galaxies of which 92 (43%) have radial velocities.

2.1 New radial velocities

The development of the Two degree Field spectrograph (2dF) on the Anglo-Australian Telescope has revolutionised cluster science. Unlike photometric surveys, spectroscopy eliminates subjective judgements of likely cluster membership based on morphology, surface brightness and colour. The purpose of the *Fornax Cluster Spectroscopic Survey, FCSS* (see Drinkwater et al. 1999) was to confirm cluster membership (to a limiting magnitude of $b_j = 19.8$) from spectral analysis of *all* 14,000 objects (both resolved and unresolved) in a 12 deg^2 region centred on NGC 1399, the optical centre of the cluster. Recent results from the first 2° diameter field are presented in Deady et al. (2002).

We have also incorporated the results from a spectroscopic survey by Drinkwater et al. (2001) of 675 bright ($16.5 < b_j < 18$) galaxies in the central $6^\circ \times 6^\circ$ region of the Fornax Cluster. Using the FLAIR-II spectrograph on the UKST at the Anglo-Australian Observatory, the purpose of this survey was to identify new cluster members which may have been misidentified 'by eye' as background objects, based on their original surface brightness classifications.

Table 1 gives details of the FCC galaxies with changed membership status resulting from both the FCSS and FLAIR-II surveys. Morphological classifications are those adopted from Drinkwater et al. (2001) where the original FCC morphologies are converted to "t-types" following the definition of de Vaucouleurs et al (1991).

Galaxies for which membership status has changed have also had their "t-type" morphological classification reassigned when appropriate. For example the previously misidentified background elliptical galaxy, FCCB1554 was confirmed by the Flair-II survey as a cluster member and is therefore more likely to be a dwarf elliptical galaxy with a -5 "t-type" classification.

Table 1. Galaxies listed in the FCC with changed membership classification.

RA	Dec (J2000)	FCC	type	bj	cz (km s ⁻¹)
03:27:33.80	-35:43:04.0	470B	S/Im	17.5	723
03:31:32.50	-35:03:43.0	729B	(d)SO	16.5	1676
03:33:43.40	-35:51:33.0	123	ImV	17.9	15483
03:33:56.20	-34:33:43.0	904B	(d)E	17.4	2254
03:33:57.20	-34:36:43.0	905B	?	17.7	1242
03:34:57.27	-35:12:23.5	141	dE4	19.2	16735 ¹
03:36:42.83	-35:26:07.7	175	dE3	17.9	31430 ¹
03:37:08.27	-34:43:52.2	189	dE4,N	19.1	31044 ¹
03:38:16.75	-35:30:27.3	1241B	dE3?	14.7	2012 ¹
03:41:03.99	-35:38:51.2	257	dE0,N?	18.4	50391 ¹
03:41:59.50	-33:20:53.0	1554B	E	17.7	1642

¹ Radial velocity taken from the FCSS. (Drinkwater et al. 2000). All other velocity measurements are taken from FLAIR-II survey (Drinkwater et al. 2001). The morphological type of each galaxy is taken from the original FCC (Ferguson 1989).

2.2 Discovery of the UCDs

A small sample of ultra-compact dwarf galaxies (UCDs) were discovered as part of the FCSS (Drinkwater et al. 1999; Deady et al. 2002). Two of the objects were previously identified by Hilker et al. (1999) in a study of the globular clusters associated with NGC 1399. Assumed to be foreground stars in earlier Fornax studies, spectral analysis of these very faint objects gives radial velocities confirming them to be cluster members. Optical imaging indicates they are unlike any other previously known cluster dwarf, with intrinsic sizes of ~ 100 pc and B band magnitudes ranging from -13 to -11 (Drinkwater et al. 2000).

The UCDs all lie within 30' of the central cD galaxy NGC 1399. The most recent investigation of NGC 1399 globular clusters (Dirsch et al. 2003) indicates that their population extends out to more than 25' at similar radii to the UCDs.

At present the origin of these enigmatic objects remains a mystery. The two most favoured hypotheses for their origin are: (1) globular cluster systems associated with the central cD galaxy NGC 1399, (2) the nuclei of tidally stripped infalling nucleated dwarf elliptical (dE,N) galaxies. Observations support various aspects of both scenarios. In either case their origin and evolution will provide a new insight into the evolution of the faint cluster population.

3 DATA AND OBSERVATIONS

Twelve 1.7 deg² CCD fields comprising the central 4° × 3° region of the Fornax Cluster were taken in photometric conditions with the CTIO Curtis Schmidt Telescope. Using a SITE 2048 × 2048 24 micron CCD each 1.3° × 1.3° field has 2.32" pixels \equiv 200 pc for d=20 Mpc (Drinkwater et al. 2001). Table 2 details the observations of each Fornax field.

Image reduction was carried out using the standard IRAF routines. Photometric calibration was achieved using the Landolt UBVR standard star catalogue (Landolt 1992). Typically two Landolt star fields from a total of four (SA92, SA98, SA95 & SA114) were observed each night, each field

Table 2. Details of the observations

Date	Field	RA	Dec (J2000)	Filter	Exp.time(s)
1995 Nov 15	NW	03:34:48	-34:26:48	B	300 × 9
				V	300 × 6
				I	300 × 6
1995 Nov 16	N	03:39:39	-34:27:05	B	540 × 5
				V	360 × 5
				I	300 × 6
1995 Nov 16	NE	03:44:30	-34:27:23	B	420 × 6
				V	360 × 5
				I	360 × 5
1995 Nov 17	E	03:42:38	-35:36:45	B	420 × 6
				V	360 × 5
				I	360 × 5
1995 Nov 17	SE	03:42:41	-36:36:45	B	420 × 6
				V	360 × 5
				I	360 × 5
1995 Nov 18	S	03:39:37	-36:27:05	B	420 × 6
				V	360 × 5
				I	360 × 5
1995 Nov 18	SW	03:34:38	-36:26:47	B	420 × 6
				V	360 × 5
				I	360 × 5
1995 Nov 19	NWW	03:27:59	-34:36:45	B	420 × 6
				V	360 × 5
				I	360 × 5
1995 Nov 19	WW	03:27:52	-35:36:45	B	420 × 6
				V	360 × 5
				I	360 × 5
1995 Nov 20	SWW	03:29:35	-36:26:19	B	420 × 6
				V	360 × 5
				I	360 × 5
1997 Jan 28	W	03:34:43	-35:26:48	B	420 × 6
				V	360 × 5
				I	360 × 5
1997 Jan 29	CORE	03:39:38	-35:27:05	B	420 × 6
				V	360 × 2
				I	360 × 5

containing 10-20 stars which were used for calibration. The photometric data are therefore on the Cousins system.

Calibration of the individual fields was carried out using the IRAF aperture photometry routines APPHOT and PHOTCAL. APPHOT was used to measure the stellar aperture magnitudes (4" radii) and PHOTCAL was used to convert to calibrated magnitudes, correcting the instrumental magnitudes for both airmass and colour. We found the colour terms for this system were not significant compared to the typical uncertainties of galaxy photometry (~ 0.1 -0.2 mag) with this data.

Sky coordinates were fitted to the individual fields for all filters. The IRAF routine CCMAP and the USNO-A V2.0 catalogue of astrometric standards were used to compute the plate solution for each image by pixel matching to celestial coordinates. The USNO-A V2.0 catalogue is favoured for its resulting accuracy in astrometry (mostly in the reduction of systematic errors) and improved photometry (the brightest stars on each plate have B and V magnitudes measured by the Tycho experiment on the Hipparcos satellite). Typical residuals for the astrometry were $\sim 0.25''$.

The images were then combined to form three 4° × 3° mosaics of the cluster in each filter (BVI). Figure 1 shows the

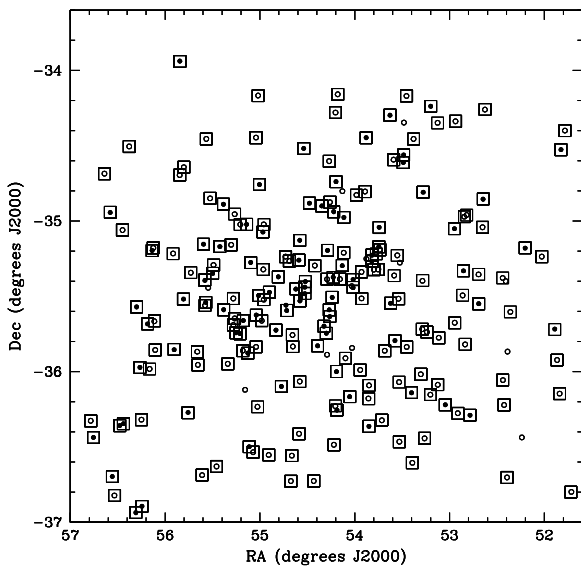


Figure 2. Distribution of cluster members in the $4^\circ \times 3^\circ$ survey area; galaxies with radial velocities (filled circles), unconfirmed members (open circles). Boxes indicate SExtractor galaxy detections in all filters (BVI).

B-band Fornax mosaic. The positions of the UCDs are also shown. For each mosaic the sky coordinates of the ‘Fornax Core’ image were used as a reference coordinate system for the entire cluster.

4 PHOTOMETRY OF CLUSTER MEMBERS

SExtractor (Source Extractor), is an automated program that optimally detects, classifies and performs photometry on sources from astronomical images (Bertin & Arnouts 1996). Using the SExtractor package we have compiled the photometry of the known Fornax Cluster members in our survey area. Their positions, magnitudes, peak surface brightness and colours were measured using SExtractor photometry routines.

Source Extraction is carried out in five main steps. An estimation of the sky background is made before a detection threshold is set. A median filter of 3×3 pixels was applied in order to suppress overestimations due to foreground stars. The images were then convolved with a Gaussian of $1.5''$ FWHM. For each mosaic image an object detection threshold was set to 2σ above the local sky background level in order to detect the faintest objects in the catalogue ($b_j \sim 19.8, 24.9$ B mag arcsec^{-2}). A minimum number of 6 connected pixels was also required for a positive detection.

Filtering of the $\sim 60,000$ SExtractor detections was achieved by matching the SExtractor catalogue to the Fornax Cluster members in the revised catalogue. All detections were confirmed by eye with obvious mis-identifications removed. Figure 2 shows the member galaxies detected from our revised catalogue.

Total magnitudes were calculated using the SExtractor MAG_BEST option, an aperture photometry routine in-

spired by Kron’s “first moment” algorithm. This routine corrects for overcrowding to which aperture photometry is sensitive (Bertin & Arnouts 1996). For isolated objects aperture magnitudes are calculated however in crowded areas where objects may overlap, an isophotal magnitude is calculated where the fraction of flux lost by the isophotal magnitude is estimated and corrected. This assumes the intensity profiles have Gaussian wings resulting from atmospheric blurring (Hilker et al. 1999).

We have used a fairly simple method for determining the central surface brightness of galaxies and have made no attempt to fit model profiles. This is partly due to the low resolution of the data as well as our attempt to reproduce the surface-brightness relation without making assumptions about galaxy morphology. Our peak surface brightness is simply calculated by determining the peak flux in the central pixel and dividing by the pixel area. As a result the surface brightness of a galaxy will be largely influenced by the seeing and our measured peak surface brightness will be an underestimate of the true central surface brightness. The measured peak surface brightness will be consistent with the true central surface brightness only for galaxies with a slow varying surface brightness at their centres, such as exponential profile galaxies with a large scale length. The implications of this will be discussed later.

B-V and V-I colours were determined using aperture photometry with $\text{radii} = 3.5r_{\text{kron}}$ which contains 99.3% of the light for galaxies with exponential profiles. Apertures defined by running the source detection algorithm on the V-band image, were then used for the B & I-band photometry. This ensures that galaxy colours are determined using identical apertures in all three filters. Table 4 contains the photometric properties of the Fornax members detected.

Photometry of the UCDs was done using the IRAF aperture photometry routines since the majority of them fell below the SExtractor detection threshold. Magnitudes and surface brightnesses were determined using the same techniques as our SExtractor photometry. The photometry of the UCDs is given in Table 3. Note that UCD2 may be suffering contamination by a foreground star. The central surface brightness is also 2 mag arcsec^{-2} brighter than those of the remaining UCD population. The colours for UCD5 are difficult to interpret. The errors on the measurements are quite large and we find a very blue V-I value given its B-V colour. The V-I colour for UCD5 is significantly bluer than that of the remaining UCDs, which have been independently measured by Mieske et al. (2002) ($\langle V-I \rangle = 1.13$). This is an unexpected result and we suspect that higher resolution observations will yield a more accurate colour measurement of this enigmatic object. The accuracy of the photometry is limited by the large pixels ($2.32''$) which makes photometry, particularly of the smallest dwarfs difficult. Our photometric errors in all bands are typically ~ 0.1 – 0.2 mag.

4.1 Selection limits

Figure 3 shows the distributions of B_T magnitudes from the FCC for the cluster members in our revised catalogue. The sample of cluster members with redshifts is limited to a magnitude of $b_j \sim 19.8$, the detection limit of the FCSS survey. Below this magnitude we assume Ferguson’s membership classifications hold.

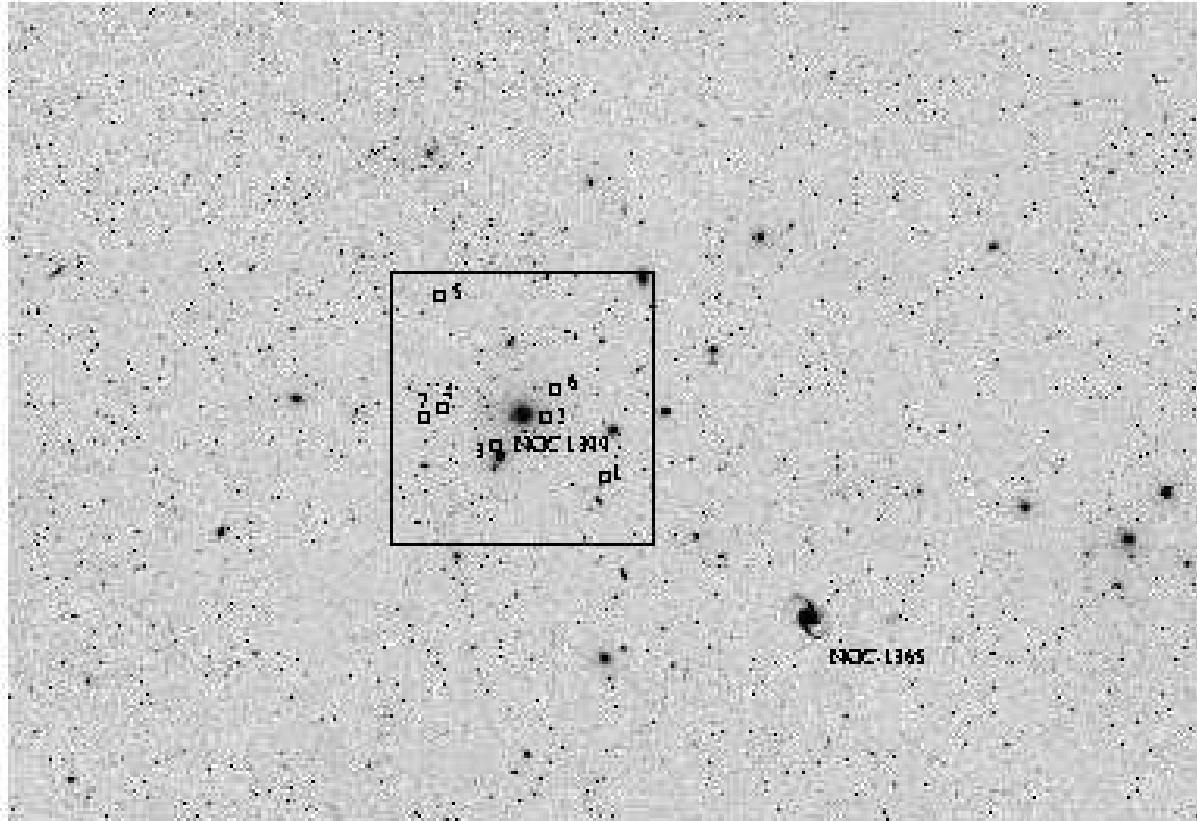


Figure 1. B-band $4^\circ \times 3^\circ$ Fornax Cluster mosaic with the distribution of the UCDs (boxes) in the central 1° region. NGC 1399 marks the optical centre of the cluster.

Table 3. Photometry of the ultra-compact dwarf galaxies discovered in the FCSS

FCSS Name (UCD#)	RA	Dec (J2000)	cz (km s^{-1})	V	$B - V$	$V - I$	μ_{Bpeak}	μ_{Vpeak}	μ_{Ipeak}
J033703.3-353804 (1)	03:37:03.30	-35:38:04.6	1481	19.3	0.9	1.2	24.9	22.2	22.1
J033806.3-352858 (2)	03:38:06.33	-35:28:58.8	1312	19.0	0.9	1.0	21.1	19.4	19.8
J033854.1-353333 (3)	03:38:54.10	-35:33:33.6	1468 ¹	17.7	1.1	1.3	23.2	21.0	20.5 ³
J033935.9-352824 (4)	03:39:35.95	-35:28:24.5	1920 ²	18.8	0.8	1.0	24.3	22.2	21.9
J033952.5-350424 (5)	03:39:52.58	-35:04:24.1	1355	19.0	1.0	0.8	25.1	22.6	22.5 ³
J033805.0-352409 (6)	03:38:05.08	-35:24:09.6	1211	18.9	0.8	1.2	23.9	21.8	21.1
J034003.4-352944 (7)	03:40:03.40	-35:29:44.0	2251	18.4	0.9	1.1	23.5	21.0	21.2

¹ CGF 1-4 and ² CGF 5-4, in Hilker et al. (1999). ³ Measurements taken using $6''$ radii apertures. All other measurements taken with $4''$ radii apertures. Colours are in the Cousins system.

Of the 213 cluster members in our revised catalogue, 92 (43%) galaxies have redshifts confirming them to be cluster members. 200 of the 213 galaxies (94%) were detected with SExtractor. Since our mosaic overlaps the fields from the FCSS, 44% of the galaxies detected (88) are confirmed members. Galaxies which were contaminated by foreground stars or suffered overcrowding have been omitted. Generally these were the faintest galaxies in the catalogue. Our final sample consists of photometry of 190 galaxies of which 85 (45%) are confirmed members. Galaxies were detected over the entire magnitude range of the catalogue to a measured apparent V magnitude of 20.5 and peak surface brightness of 24.9 (V mag arcsec^{-2}).

5 SURFACE BRIGHTNESS - MAGNITUDE RELATION

It has been well established (Ferguson & Sandage 1988; Ferguson & Binggeli 1994) that there exists an empirical surface brightness-magnitude relation for normal elliptical and dwarf galaxy populations. The physical basis of this relation is not well understood and many authors have suggested that it is simply a manifestation of the methods in which galaxy samples are selected (Phillipps et al. 1987, 1988).

In this section we discuss the surface brightness-magnitude relation and its use for determining cluster mem-

Table 4. Photometry of Fornax Cluster members

FCC	RA	Dec (J2000)	V_{best}	μV_{peak}	B_{best}	μB_{peak}	I_{best}	μI_{peak}	$B - V$ ¹	$V - I$ ¹	"t-type"
52	3:27:08.14	-34:23:59.3	18.17	23.88	18.89	24.74	16.60	22.95	0.68	1.09	-5
55	3:27:18.05	-34:31:33.9	12.91	19.38	14.04	20.34	11.46	18.37	0.93	1.43	-1
56	3:27:21.61	-36:08:47.2	17.08	23.25	17.81	23.86	15.92	22.28	—	—	-5
57	3:27:27.91	-35:55:24.5	17.16	22.90	17.79	23.48	16.26	22.04	0.51	0.99	-5
65	3:28:06.68	-35:14:11.7	16.98	22.79	17.75	23.48	16.01	21.86	0.66	1.00	-5
67	3:28:48.77	-35:10:49.1	13.37	20.93	14.15	21.93	12.13	19.62	0.79	1.24	5
71	3:29:26.30	-35:36:13.3	19.08	24.72	—	—	—	—	—	—	-5
73	3:29:34.53	-36:42:10.8	19.12	24.52	20.09	24.75	18.22	23.80	—	—	-5
77	3:29:42.00	-36:13:12.2	17.98	23.42	18.55	24.68	17.07	23.05	0.69	1.02	-5
78	3:29:45.47	-35:22:42.4	18.56	24.48	—	—	—	—	0.61	1.18	-5
82	3:30:30.52	-34:15:36.0	15.87	22.17	16.69	22.88	14.79	21.10	0.77	1.10	-5
83	3:30:35.19	-34:51:19.2	11.35	17.13	12.30	18.56	10.11	16.16	0.92	1.24	-4
84	3:30:36.64	-35:02:29.3	18.76	24.37	19.51	24.59	17.19	22.68	—	—	-5
85	3:30:46.21	-35:32:57.9	15.65	22.07	16.43	22.98	14.61	21.12	0.81	1.13	-5
86	3:30:46.68	-35:21:15.9	17.12	23.18	—	—	—	—	0.76	1.18	-5
90	3:31:08.21	-36:17:24.2	14.19	19.33	14.82	19.84	13.16	18.81	—	—	-4
92	3:31:16.86	-34:57:37.7	18.66	24.51	—	—	—	—	—	—	10
93	3:31:20.75	-35:49:09.9	18.97	24.69	—	—	17.87	23.50	—	—	-5
94	3:31:22.84	-34:58:18.0	19.03	24.68	19.85	25.10	17.18	23.53	—	—	-5
95	3:31:24.83	-35:19:51.1	14.02	20.14	14.90	21.11	12.85	19.10	0.85	1.18	-1
97	3:31:26.90	-35:29:40.3	18.65	24.55	—	—	—	—	—	—	-5
98	3:31:39.17	-36:16:35.0	18.41	24.49	—	—	18.22	23.55	—	—	10
99	3:31:44.90	-34:20:17.3	16.58	23.19	17.41	23.85	15.73	22.25	0.72	0.97	-5
101	3:31:46.90	-35:40:32.4	16.56	22.76	17.17	23.72	—	—	—	—	-5
100	3:31:47.67	-35:03:05.5	14.86	21.84	15.75	22.65	13.72	20.79	0.85	1.13	-5
102	3:32:10.73	-36:13:13.8	15.97	22.49	16.42	22.88	15.00	21.86	—	—	10
103	3:32:27.38	-35:46:30.8	19.80	24.35	—	—	18.35	23.76	—	—	-5
105	3:32:29.93	-36:05:17.0	17.60	23.77	17.13	24.43	16.19	22.78	—	—	-5
104	3:32:30.36	-34:20:52.9	—	—	19.16	24.43	—	—	—	—	-5
106	3:32:47.77	-34:14:18.9	14.52	20.07	15.49	21.16	13.40	19.05	0.97	1.12	-1
108	3:32:48.69	-36:09:11.0	19.12	24.54	18.86	24.90	18.12	23.48	—	—	-5
110	3:32:57.37	-35:44:15.5	16.69	23.17	17.39	24.15	15.25	22.23	0.75	1.23	-5
112	3:33:03.34	-36:26:35.9	16.67	23.12	17.29	23.83	15.73	22.25	0.64	1.02	-5
113	3:33:06.83	-34:48:31.7	14.83	21.71	15.51	22.42	13.84	20.87	0.66	0.98	5
115	3:33:09.27	-35:43:05.2	16.31	22.79	16.71	23.17	15.34	22.17	0.41	0.91	8
116	3:33:12.83	-36:01:02.4	15.77	22.06	16.46	22.77	14.69	21.13	0.80	1.05	-5
118	3:33:31.29	-34:27:19.5	17.28	23.40	18.14	24.15	16.45	22.54	—	—	-5
120	3:33:34.24	-36:36:19.7	15.99	22.74	16.46	23.04	15.04	22.04	0.44	0.95	10
121	3:33:36.31	-36:08:27.8	9.31	17.54	10.23	18.55	8.18	16.13	0.65	1.14	4
125	3:33:48.52	-35:50:09.5	18.95	24.17	19.82	24.89	17.28	23.53	—	—	-5
124	3:33:49.04	-34:10:10.5	17.85	23.92	18.80	24.40	16.97	23.04	—	—	-5
904	3:33:56.20	-34:33:43.0	16.66	21.86	17.57	22.75	15.60	21.01	0.89	1.05	-5
905	3:33:57.20	-34:36:40.0	16.83	22.41	17.53	23.22	15.93	21.87	0.73	0.96	10
128	3:34:07.07	-36:27:56.6	16.35	22.42	16.94	22.89	15.50	21.69	0.54	1.00	10
129	3:34:07.74	-36:04:10.7	19.21	24.51	—	—	—	—	—	—	10
130	3:34:09.23	-35:30:59.7	18.99	24.58	—	—	16.70	23.52	—	—	10
131	3:34:12.23	-35:13:40.9	20.30	24.42	—	—	18.92	23.66	—	—	-5
132	3:34:18.31	-35:47:40.3	17.91	23.12	18.78	23.85	16.86	22.18	0.87	0.99	-5
133	3:34:20.22	-35:21:43.4	—	—	17.70	24.10	—	—	—	—	-5
134	3:34:21.80	-34:35:33.4	17.09	22.58	17.97	23.35	15.96	21.75	—	—	-5
136	3:34:29.54	-35:32:45.9	14.17	20.55	15.02	21.58	13.04	19.58	0.82	1.13	-5
135	3:34:30.89	-34:17:51.0	15.11	21.26	16.00	22.32	14.00	20.28	0.89	1.10	-5
137	3:34:44.16	-35:51:40.8	17.26	23.64	17.40	24.61	16.42	22.80	0.39	0.99	-5
140	3:34:56.49	-35:11:27.5	18.43	24.08	19.20	24.85	16.96	23.25	0.66	1.05	-5
142	3:34:58.30	-35:02:32.6	18.21	24.06	19.50	25.08	17.01	23.17	—	—	-5
143	3:34:59.21	-35:10:14.6	13.38	18.51	14.28	19.65	12.19	17.56	0.89	1.19	-4
144	3:35:00.30	-35:19:19.7	18.82	24.06	19.82	24.75	17.82	23.45	—	—	-5
145	3:35:05.54	-35:13:06.0	—	—	18.77	24.76	—	—	—	—	-5
146	3:35:11.58	-35:19:22.4	19.48	24.24	20.37	24.89	18.67	23.58	—	—	-5
147	3:35:16.90	-35:13:38.7	11.07	17.19	12.03	18.37	9.82	16.14	0.93	1.25	-4
148	3:35:16.94	-35:16:00.7	12.32	18.15	13.22	19.05	11.18	17.30	0.82	1.15	-1
149	3:35:23.85	-36:05:29.1	20.07	24.97	—	—	14.00	19.59	—	—	-5
150	3:35:24.06	-36:21:49.2	15.13	20.55	15.86	21.44	19.16	23.49	0.74	1.12	-5
151	3:35:25.42	-36:10:43.2	17.48	22.75	17.95	23.90	16.27	21.26	—	—	-5
153	3:35:31.06	-34:26:49.5	12.27	18.39	13.35	19.66	11.04	17.38	1.07	1.22	-1
155	3:35:33.96	-34:48:16.7	18.21	23.64	19.06	24.60	17.22	22.81	—	—	-5
156	3:35:42.79	-35:20:17.2	17.99	23.34	19.32	24.37	16.85	22.37	—	—	-5
157	3:35:42.84	-35:30:50.2	16.89	23.43	17.72	24.27	15.82	22.52	0.71	1.20	-5
158	3:35:46.35	-35:59:22.4	16.27	23.00	17.02	23.86	15.40	22.10	0.71	1.09	-5
159	3:35:55.68	-34:49:39.9	18.16	24.03	19.42	25.05	17.17	23.49	—	—	-5
160	3:36:04.07	-35:23:19.5	16.89	22.01	17.72	23.59	15.78	20.38	—	—	-5
161	3:36:04.10	-35:26:34.5	11.10	17.67	12.04	18.90	9.87	16.60	0.92	1.23	-4
164	3:36:12.94	-36:09:59.0	15.83	21.50	16.50	22.33	14.74	20.56	0.71	1.08	-5
165	3:36:23.59	-35:54:40.6	17.09	23.39	17.76	24.14	16.08	22.56	—	—	-5
167	3:36:27.61	-34:58:35.8	10.05	17.05	11.09	18.30	8.78	16.02	1.03	1.26	0
168	3:36:27.88	-35:12:37.9	18.68	24.14	19.20	24.80	17.23	22.95	—	—	-5
170	3:36:31.75	-35:17:48.1	11.50	17.17	12.46	18.31	10.24	16.01	0.95	1.25	-1
171	3:36:37.51	-35:23:09.4	18.15	23.83	19.34	24.47	16.85	23.17	—	—	-5
173	3:36:43.12	-34:09:32.7	17.68	23.36	18.70	24.39	16.60	22.50	—	—	-5
176	3:36:45.14	-36:15:21.9	12.15	19.24	12.32	20.44	11.37	18.52	—	—	1
179	3:36:46.41	-36:00:02.0	11.16	17.16	12.02	18.34	9.94	16.16	0.86	1.23	1
177	3:36:47.50	-34:44:21.0	12.57	18.96	13.63	20.12	11.37	18.06	1.04	1.19	-1
178	3:36:48.64	-34:16:48.0	16.75	23.06	17.60	23.97	15.66	22.05	0.82	1.07	-5
183	3:36:52.89	-36:29:10.4	16.76	22.91	17.36	23.73	15.60	22.02	0.71	1.07	-5
181	3:36:53.21	-34:56:17.3	17.04	22.78	17.56	23.65	16.05	21.87	0.59	1.00	-5
182	3:36:54.39	-35:22:27.4	14.07	19.53	14.95	20.64	12.91	18.70	0.88	1.16	-1
184	3:36:57.00	-35:30:28.6	10.67	16.78	11.66	18.01	9.37	16.11	0.98	1.29	-1
185	3:37:02.78	-34:52:30.9	19.44	24.37	—	—	18.18	23.52	—	—	-5
188	3:37:04.66	-35:35:24.0	16.41	21.66	16.96	23.01	14.49	21.00	0.64	0.94	-5
187	3:37:04.86	-34:36:11.0	15.62</td								

Table 5. (cont'd) Photometry of Fornax Cluster members

FCC	RA	Dec (J2000)	V_{best}	μ_{Vpeak}	B_{best}	μ_{Bpeak}	I_{best}	μ_{Ipeak}	$B - V$ ¹	$V - I$ ¹	"t-type"
196	3:37:33.96	-35:49:44.8	17.17	23.31	17.79	24.02	16.17	22.35	0.62	1.18	-5
197	3:37:41.01	-35:17:46.2	18.91	23.95	19.71	25.18	18.51	23.44	-	-	-5
199	3:37:43.73	-36:43:35.4	18.22	24.13	19.13	24.74	17.38	23.50	0.69	0.97	10
200	3:37:54.77	-34:52:55.0	16.85	22.64	17.37	23.15	15.71	21.95	0.49	0.96	-5
202	3:38:06.55	-35:26:22.7	14.01	20.49	11.63	19.92	-	-	0.86	1.19	-4
203	3:38:09.25	-34:31:05.8	14.78	21.09	15.28	21.78	13.86	20.31	0.50	0.94	-5
208	3:38:18.80	-35:31:49.4	16.58	22.70	16.84	23.52	15.63	21.85	0.59	0.98	-5
210	3:38:19.22	-36:03:56.5	18.79	23.95	19.14	24.72	14.22	20.14	0.53	1.11	-5
207	3:38:19.27	-35:07:43.4	15.30	21.05	16.10	21.88	17.64	23.25	0.79	1.06	-5
212	3:38:21.01	-36:24:47.6	16.93	23.48	18.05	24.28	16.36	22.74	-	-	-5
211	3:38:21.48	-35:15:34.6	15.77	20.97	16.52	21.80	14.71	20.15	0.75	1.06	-4
213	3:38:29.29	-35:27:07.0	9.32	16.59	10.77	17.69	-	-	-	-	-4
214	3:38:36.62	-35:50:01.5	18.95	23.74	19.21	24.51	17.57	23.25	0.51	0.10	-5
215	3:38:37.63	-35:45:24.6	19.45	24.35	19.97	24.91	18.60	23.53	0.61	0.97	-5
216	3:38:39.26	-36:33:28.7	18.23	24.47	19.56	24.56	16.54	23.24	-	-	-5
217	3:38:41.61	-36:43:36.8	19.50	24.49	20.38	24.90	18.25	23.37	-	-	-5
218	3:38:45.42	-35:15:57.0	18.15	23.80	18.69	24.45	17.05	22.96	0.59	1.17	-5
219	3:38:52.24	-35:35:42.4	9.92	16.39	10.88	17.48	8.66	15.91	0.97	1.25	-4
220	3:38:55.15	-35:14:11.6	18.11	23.98	19.39	25.00	16.42	23.21	-	-	-5
221	3:39:05.78	-36:05:55.2	17.13	22.44	17.76	23.21	16.15	21.53	0.63	1.05	-5
222	3:39:13.42	-35:22:15.7	14.03	21.54	15.52	22.34	12.86	20.50	0.93	1.30	-5
227	3:39:50.23	-35:31:20.9	19.40	24.42	19.85	24.61	17.35	23.55	-	-	-5
226	3:39:50.24	-35:01:20.8	-	-	-	-	18.42	23.48	-	-	-5
228	3:39:51.41	-35:19:18.9	18.96	24.12	-	-	18.35	23.57	-	-	-5
229	3:39:55.31	-35:39:44.2	18.24	24.28	19.19	24.59	17.69	23.33	-	-	-5
230	3:40:01.30	-34:45:28.5	16.80	22.35	17.14	22.89	15.84	21.54	0.39	0.93	-5
231	3:40:04.62	-34:10:02.7	17.80	23.19	18.31	24.33	16.89	22.41	-	-	-5
233	3:40:06.26	-36:14:00.8	-	-	19.89	24.83	-	-	-	-	10
236	3:40:09.93	-35:50:10.1	18.34	24.04	18.93	24.77	-	-	-	-	-5
234	3:40:10.02	-34:26:46.0	16.60	23.29	17.12	23.78	15.80	22.57	0.48	0.80	-5
238	3:40:17.19	-36:32:05.5	17.97	23.81	19.23	24.77	17.16	22.97	-	-	-5
241	3:40:23.41	-35:16:32.8	16.22	22.89	16.96	23.70	15.30	21.91	0.75	1.01	-5
243	3:40:27.02	-36:29:56.1	15.81	22.09	16.62	22.90	14.79	21.07	0.79	1.05	-5
244	3:40:30.73	-35:52:39.3	17.69	23.16	18.44	23.85	16.36	21.42	-	-	-5
245	3:40:33.86	-35:01:21.4	15.37	21.72	15.94	22.45	14.40	20.90	0.60	1.05	-5
247	3:40:42.32	-35:39:40.0	17.67	23.63	18.00	23.75	17.08	23.00	-	-	-5
248	3:40:43.43	-35:51:39.0	18.40	23.30	19.05	24.00	17.13	22.46	0.69	1.14	-5
251	3:40:49.62	-35:01:24.4	18.79	24.37	18.86	24.95	17.86	23.52	-	-	-5
252	3:40:50.38	-35:44:53.5	15.32	21.16	16.22	22.17	14.18	20.26	0.89	1.152	-5
254	3:41:00.77	-35:44:31.1	16.59	23.09	18.04	23.85	16.10	22.35	-	-	-5
256	3:41:03.80	-34:57:16.2	19.23	24.60	-	-	-	-	-	-	-5
258	3:41:07.13	-35:41:24.4	20.70	24.63	-	-	18.18	23.37	-	-	-5
259	3:41:07.48	-35:30:53.5	17.58	23.69	18.51	24.65	17.24	22.77	-	-	-5
260	3:41:12.79	-35:09:29.8	16.67	22.88	17.34	23.84	15.79	22.14	0.66	0.86	-5
262	3:41:21.42	-35:56:54.3	17.44	23.64	18.04	24.24	16.01	21.47	-	-	-5
264	3:41:31.83	-35:25:20.9	16.23	21.89	16.92	22.60	15.16	21.09	0.70	1.02	-5
263	3:41:32.33	-34:53:21.9	13.39	19.75	13.65	19.93	12.60	19.18	-	-	6
266	3:41:41.31	-35:10:12.5	15.72	20.91	16.02	21.90	14.16	19.91	0.79	1.17	-5
268	3:41:49.86	-36:37:48.1	18.50	23.53	19.43	24.44	-	-	-	-	-5
269	3:41:57.41	-35:17:31.4	18.17	24.06	-	-	17.24	22.64	0.70	1.14	-5
1554	3:41:59.50	-35:20:53.0	16.23	21.89	-	-	14.98	20.85	0.90	1.29	-5
271	3:42:06.23	-34:50:58.0	18.43	23.86	19.29	24.57	17.24	23.29	0.67	1.01	-5
273	3:42:15.77	-34:27:17.5	18.04	23.84	19.15	24.20	17.48	22.88	0.60	0.98	-5
274	3:42:17.31	-35:32:25.7	16.01	21.82	16.54	22.84	15.02	21.26	0.65	0.99	-5
275	3:42:18.98	-35:33:38.7	-	-	18.56	24.79	17.64	23.38	-	-	-5
276	3:42:19.32	-35:23:40.8	10.86	17.07	11.77	18.21	9.64	16.05	0.89	1.22	-4
277	3:42:22.76	-35:09:15.0	12.65	17.60	13.50	18.63	11.52	16.91	0.84	1.14	-4
279	3:42:26.40	-36:41:13.2	16.27	23.06	16.73	23.71	15.13	21.96	0.59	1.10	-5
280	3:42:36.96	-35:57:20.9	18.24	24.13	19.17	24.71	17.29	23.24	0.75	0.98	-5
281	3:42:38.69	-35:52:03.9	17.59	23.69	18.35	24.46	16.55	22.72	0.77	1.07	-5
284	3:42:54.92	-35:20:35.9	18.89	24.44	-	-	18.00	23.67	0.54	1.05	-5
285	3:43:01.95	-36:16:16.4	13.78	21.72	14.24	22.20	12.90	20.86	0.41	0.89	7
286	3:43:12.69	-34:38:35.0	17.68	23.06	18.23	23.90	16.58	21.90	0.71	1.08	-5
287	3:43:13.53	-35:31:07.0	17.52	23.37	18.45	24.09	16.52	22.43	0.77	1.06	-5
288	3:43:22.77	-33:56:19.5	14.94	20.78	15.69	21.72	13.80	19.77	0.75	1.14	-5
289	3:43:23.20	-34:41:42.6	18.10	24.07	18.68	24.55	17.15	23.27	0.65	0.94	-5
290	3:43:37.09	-35:51:17.5	11.52	19.45	12.36	20.34	10.51	18.44	-	-	5
291	3:43:39.72	-35:12:56.6	19.26	24.29	-	-	-	-	-	-	-5
293	3:44:25.19	-35:51:23.4	17.10	23.02	17.96	23.80	15.84	22.32	0.72	1.09	-5
295	3:44:29.98	-35:10:41.6	18.32	23.99	18.45	24.53	17.03	23.26	0.45	0.98	-5
296	3:44:32.94	-35:11:44.8	15.75	21.60	16.46	22.53	14.71	20.62	0.70	1.06	-5
297	3:44:39.28	-35:58:57.2	-	-	-	-	16.44	23.12	-	-	-5
298	3:44:44.41	-35:41:00.5	16.02	21.39	16.76	22.32	14.92	20.55	0.74	1.08	-5
299	3:44:58.67	-36:53:40.4	16.42	22.44	16.95	22.97	15.42	21.57	0.51	0.10	7
300	3:44:59.94	-36:19:09.5	15.38	22.56	16.23	23.40	14.29	21.45	0.81	1.13	-5
301	3:45:03.65	-35:58:21.7	13.19	18.66	14.04	19.68	12.01	17.66	0.83	1.18	-4
302	3:45:12.32	-35:34:14.2	15.46	21.83	15.59	21.99	14.89	21.92	-	-	8
303	3:45:14.08	-36:56:12.4	15.06	21.20	15.84	22.09	13.99	20.29	0.76	1.11	-5
304	3:45:30.83	-34:30:18.3	17.97	24.50	19.51	24.56	17.25	23.57	-	-	-5
306	3:45:45.41	-36:20:45.2	15.66	21.16	21.51	21.78	17.55	-	-	-	9
307	3:45:47.80	-35:03:37.3	17.08	24.33	17.81	24.45	15.93	22.22	0.69	0.10	-5
308	3:45:54.87	-36:21:29.8	13.10	20.66	13.90	21.42	11.91	19.56	0.72	1.18	7
309	3:46:08.24	-36:49:21.7	18.45	24.47	-	-	16.68	23.60	-	-	-5
310	3:46:13.82	-36:41:48.0	12.60	19.18	13.46	20.19	11.36	18.13	0.86	1.21	-1
312	3:46:19.01	-34:56:36.2	11.74	19.66	12.46	20.51	10.59	18.45	0.71	1.16	5
313	3:46:33.45	-34:41:09.1	16.84	22.74	17.64	23.36	15.75	21.73	0.72	1.11	-5
316	3:47:01.52	-36:26:14.9	15.82	22.51	16.80	23.38	14.75	21.56	0.87	1.08	-5
318	3:47:08.17	-36:19:36.3	15.54	22.45	16.41	23.31	14.60	21.49	0.79	1.04	-5

¹ Colours are in the Cousins system.

bership. We also present the relation for our sample of Fornax Cluster galaxies, paying particular attention to the location of the ultra-compact dwarf galaxies. Our surface brightness relation spans a luminosity range over four magnitudes, to a limit of $b_j \sim 19.8$. Unlike previous studies which have concentrated on

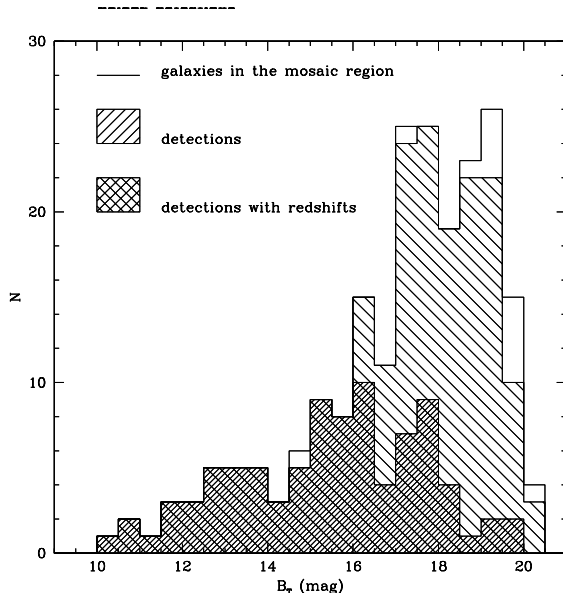


Figure 3. Distribution of B_T magnitudes (FCC) of catalogue members and SExtractor detections. Solid line represents galaxy members in our catalogue of the central $4^\circ \times 3^\circ$ region. The hatched histogram indicates the galaxies detected. The cross-hatched histogram indicates the proportion of galaxies with radial velocities.

5.1 Cluster membership

The greatest problem concerning the study of the faint cluster population is distinguishing members from the background population. Few clusters have known radial velocities of their faintest members. The 2dF and Flair-II Fornax Cluster surveys provide the largest sample of confirmed faint members. In this section we investigate the surface brightness-magnitude relation for members and non-members and its application to cases where radial velocities may be unobtainable.

Figure 4 is the surface brightness relation for Fornax Cluster members and background galaxies in the region defined by our mosaic. Unconfirmed background galaxies from the FCC are plotted as points and unconfirmed members as circles. Confirmed cluster members with redshifts determined from the FCSS and Flair-II surveys are plotted as filled circles and background galaxies as crosses.

Members and background galaxies exhibit strong surface brightness relations, background galaxies having a higher central surface brightness for a given magnitude. The dashed line separates the two populations; member galaxies occupy the region to the left. This separation between the relations has been optimised such that the minimum number of confirmed background galaxies would be classified as cluster members. Of the 224 galaxies to the left of the dashed line only 6% are confirmed background galaxies.

We detected three background galaxies from the FCC which from the Flair-II survey, were found to be cluster members. Their location on the surface brightness magnitude plot places them clearly within the cluster member population. Similarly, we detected all four of the new background galaxies, confirmed by the FCSS observations. Three

of these lie well within the population of background galaxies.

For surface brightnesses $< 21.5 \text{ mag arcsec}^{-2}$ the separation between populations is obvious however as surface brightness increases distinguishing between background and member galaxies becomes more difficult. In this regime a higher proportion of background galaxies may masquerade as cluster members and vice versa. The inability of the surface brightness relation to characterise the faintest cluster members is entirely due to the resolution and seeing of the data. This effect and its implications will be left to the discussion.

The small sample of galaxies to the right of the background sample are the ultra-compact dwarf galaxies (UCDs). These high surface-brightness galaxies occupy the intermediate region between the cluster dwarf population and galactic globular clusters (Ferguson & Binggeli 1994). In this case membership judgements based on surface brightness and luminosity break down and radial velocities are needed to determine membership.

5.2 Surface brightness-magnitude relation for cluster members

Our sample of 190 member galaxies covers a wide range of morphological types. Figure 5 shows the surface brightness relation for the entire sample in all bands. The surface brightness relation for Fornax galaxies follows a narrow locus and as expected late-type galaxies tend to have a lower surface brightness for a given magnitude.

The UCDs lie in an isolated region in the surface brightness-magnitude diagram suggesting they form a distinct class of object. Their luminosities overlap the faint end of the dwarf population, $-13 < M_B < -11$, based on a distance modulus of 31.5 (Drinkwater et al. 2001). However lower limits of their surface brightness ($\sim 22.4 \text{ mag arcsec}^{-2}$) suggest core luminosities much brighter than any other Fornax Cluster dwarf of the same magnitude. They are also brighter than any of the globular clusters associated with NGC 1399, the most luminous globular having an absolute magnitude of $M_B \sim -11$ (Forbes et al. 1998).

The observed gap between the E and dE galaxies at an absolute magnitude of $B \sim -17$ is consistent with the results of Ferguson & Binggeli (1994). The dichotomy is progressively less pronounced as you move to redder wavelengths. The V and I-band relations show a fairly smooth transition between the dwarf and elliptical populations. A similar result has been recently obtained by Graham & Guzman (2003) from HST photometry of dE galaxies and bright E galaxies in Coma.

The population of elliptical galaxies follow a fairly well defined sequence with central surface brightness increasing with decreasing luminosity, with similar scatter as the dE galaxies. This is the opposite trend to the results of Kormendy (1985); Graham & Guzman (2003), and we suspect it is due to the fact that we are not resolving the cores of the galaxies. This will be discussed in more detail in section 7.

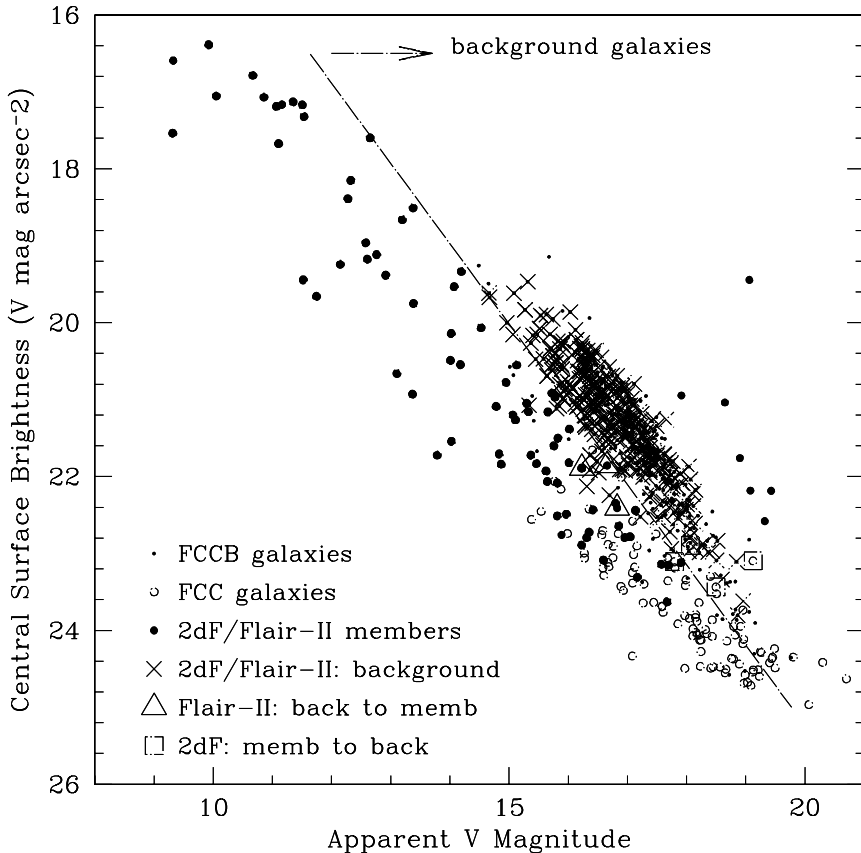


Figure 4. Surface brightness-magnitude diagram for cluster members and background galaxies. Cluster members (from FCC): unconfirmed (open circles), confirmed by Flair-II/2dF (filled circles). Background galaxies (from FCCB): unconfirmed (points), confirmed by Flair-II (crosses). Triangles are Flair-II confirmed members originally classified as background galaxies. Squares are 2dF confirmed background galaxies originally classified as cluster members. The dashed line represents the segregation between populations ($SB = 1.06 V + 4.16$)

6 COLOUR ANALYSIS OF CLUSTER GALAXIES

We have determined B-V and V-I colours for 113 cluster galaxies. Reddening is very small towards Fornax ($E_{(B-V)} \simeq 0.01$ mag, Schlegel et al. (1998)) and can be neglected in interpreting the results. The colour-magnitude plot for the entire population is shown in figure 6. Again we adopt the “t-type” classification scheme described above.

The colour-magnitude properties of galaxies are an important aspect of galaxy evolution studies. The well known colour-magnitude relation for bright cluster ellipticals (Terlevich et al. 2001; Visvanathan & Sandage 1977; Vazdekis et al. 2001) is generally attributed to a metallicity effect. More massive galaxies tend to have higher metallicities as a result of their large binding energies, appearing redder than the less massive galaxies.

Our data show that early-type galaxies become progressively redder with increasing luminosity. Galaxies classified as SO/a morphological types also follow the same colour-magnitude relation as elliptical galaxies. A least squares fit to the E and SO population gives a slope of -0.034 ± 0.006 . This is consistent with the observations of Griersmith (1982)

who find a slope of -0.038 ± 0.005 for both Fornax and Virgo elliptical and SO populations. The V-I colour magnitude relation gives a similar result. A least squares fit to the data yields: $(V-I) = -0.028V + 1.52$ with an RMS of 0.8. Hilker et al. (2003) find a similar result for their study of dwarf spheroidals in Fornax.

The relation for early-type galaxies is fairly tight which is expected for bright cluster galaxies. In contrast, luminous late-type galaxies show a much broader distribution and as expected are significantly more blue. This is a similar result to that found in other clusters, for example in Coma (Terlevich et al. 2001) and reflects the different star-formation histories.

The colour-magnitude properties of dwarf galaxies in the Fornax Cluster have been discussed by many authors (Evans et al. 1990; Phillipps et al. 1987). The dE and dE,N populations follow a colour-magnitude relation in the sense that the brighter dE and dE,N galaxies are redder. A similar result was also obtained by Caldwell & Bothun (1987) and Hilker et al. (1999). Our results are consistent with previous studies and we find that both dE and dE,N galaxies follow the same colour-magnitude relation. As expected the scat-

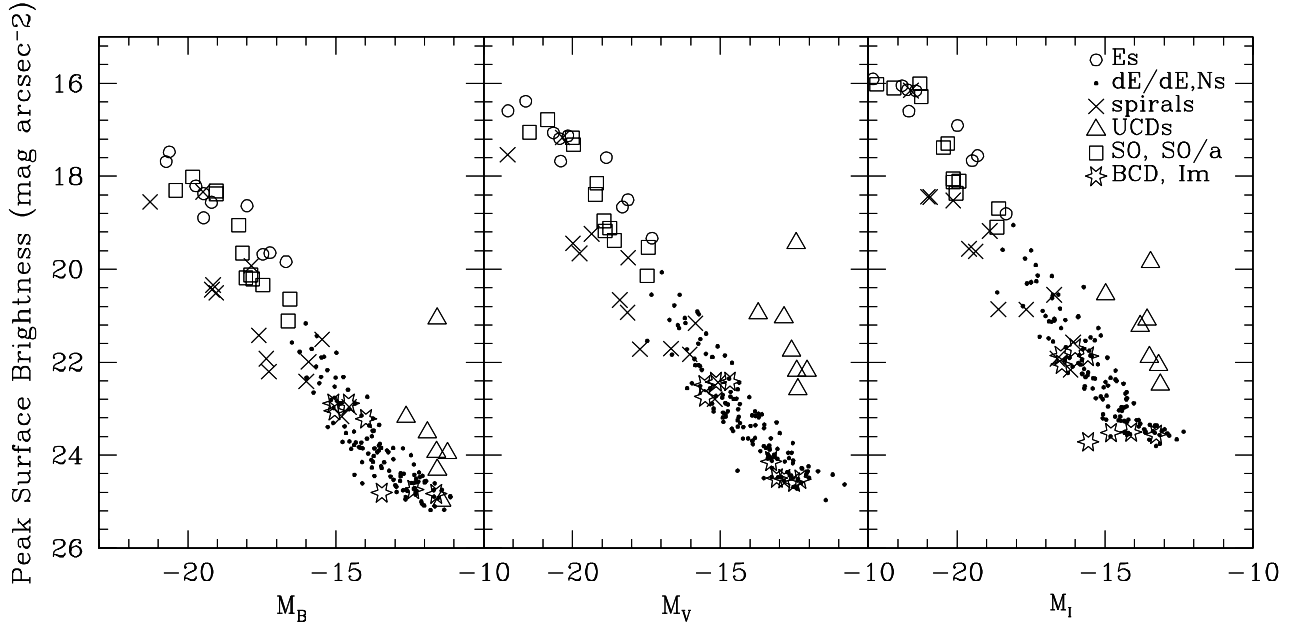


Figure 5. Magnitude-surface brightness diagram for Fornax Cluster members. A discontinuity between the E and dE populations is observed in the B band relation.

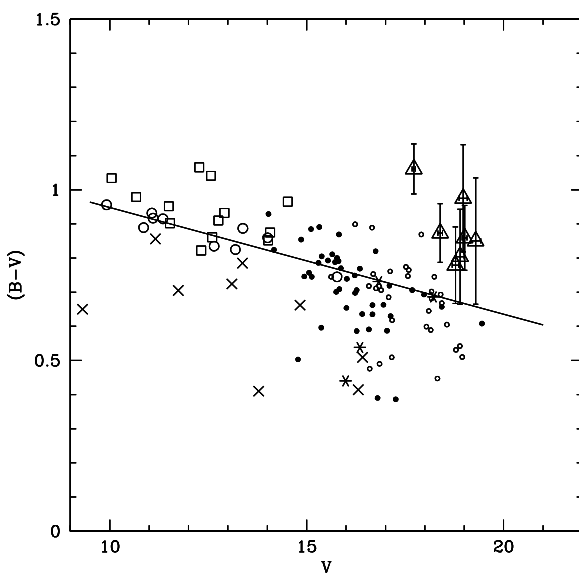


Figure 6. Colour-magnitude plot of cluster members; circles-Es, boxes-SO/a, small circles-dE, filled circles-dE,Ns from the FCC, crosses-spirals, asterix-BCD/Im and triangles-UCDs. Colours are in the Cousins system. The solid line represents a least-squares fit to the ellipticals.

ter increases towards the faint end of the population and bluerward of the relation for early-type galaxies.

By contrast, the UCD galaxies lie significantly above the colour-magnitude relation for early-type galaxies although the amount of scatter redward of the relation for ellipticals is comparable to the bluest dwarfs. Previous photometric studies of dE,N galaxies suggest that there is no measurable difference between the colours of their cores and halos (Caldwell & Bothun 1987). With the exception of the brightest, the location of the UCDs on the colour-magnitude is therefore consistent with the galaxy threshing model of a bright dE,N galaxies (Bekki et al. 2001). As the halo of the dE,N is stripped and the luminosity decreases the colour of the galaxy core remains the same. We would expect the remnant nuclei, UCD to be shifted off the locus of the the colour-magnitude relation.

The histograms in Figure 7 show the colour distribution of the dwarf population, separated by their morphologies or “t-types”. The dwarf elliptical population has been further divided into nucleated and non-nucleated using the original classification by Ferguson (Ferguson 1989).

The mean colours of each population are also given in Table 6. Using K_S - and t -tests we find that the distribution and mean B-V colours of the UCDs are significantly different from the ‘normal’ dE population, at the 99% confidence level. The UCDs are redder than the dE and dE,N ($\langle B-V \rangle = 0.7$) population having a $\langle B-V \rangle$ colour of 0.89. Their V-I colours, $\langle V-I \rangle = 1.09$, are consistent with the colours of galactic globular clusters of the Harris Catalogue (Harris 1996). They are also typical of the globular clusters of NGC

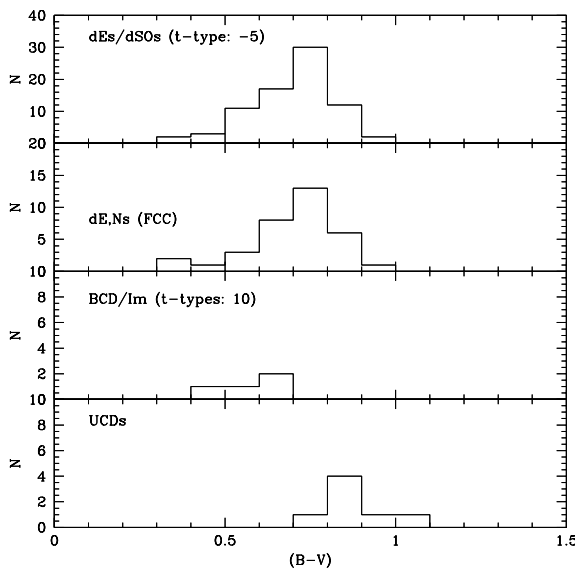


Figure 7. Histograms of the B-V colours of Fornax dwarf; dE,Ns classified by Ferguson have been separated from the dE population based on the t-type scheme.

Table 6. Mean B-V & V-I colours of the dwarf population

Sample	n	$\langle B-V \rangle, \sigma$	$\langle V-I \rangle, \sigma$
dEs/dS0s (t-types: -5)	76	0.70, 0.12	1.06, 0.08
dE,Ns (FCC)	34	0.71, 0.13	1.06, 0.09
BCD/Im (t-types: 10)	4	0.57, 0.10	1.02, 0.10
UCDs	7	0.89, 0.12	1.09, 0.14

Note: Colours are in the Cousins system.

1399 (Kissler-Patig et al. 1997; Dirsch et al. 2003). Our results are consistent with the most recent published colours of Mieske et al. (2002).

Bothun et al. (1991) also investigated the colours of a small sample of LSB Fornax galaxies. Their sample of dE galaxies were found to be relatively blue with a $\langle B-V \rangle$ of 0.6. Since there is a trend for photographically selected LSB galaxies to be blue (Impey et al. 1988) their result was interpreted to be partially due to selection effects. The mean for our sample of dwarf galaxies is ($\langle B-V \rangle = 0.69$) which is consistent within errors to the results of Bothun et al. (1991).

As expected, late-type dwarfs are bluer ($\langle B-V \rangle = 0.57$) than early type dwarfs, reflecting the relative star formation histories of the populations.

7 DISCUSSION

7.1 Membership

Previous photographic studies of galaxy clusters have relied on a multitude of techniques used to distinguish cluster members from background galaxies. These include statistical methods based on colour selection, morphology and surface

brightness measurements and in most cases this has proved to be adequate for the study of cluster populations.

In a study of the Virgo cluster, Sandage & Binggeli (1984) concentrated on the more complicated identification of low-luminosity dwarf galaxies. These were judged to be cluster members either from their uniquely low surface brightnesses and/or morphological classifications. The Fornax Cluster Catalogue (Ferguson 1989) was also constructed using the same technique. From the results of more recent spectroscopic surveys of the Fornax Cluster only a small percentage of galaxies in the FCC were assigned incorrect membership classifications.

The motivation of our investigation was to test whether the empirical surface brightness relation is simply a result of the way galaxy samples are chosen. Our sample is based on the results of the Fornax Cluster Spectroscopic Survey and the Flair-II Fornax survey in order to obtain as many cluster and background galaxies with confirmed redshifts. We have assumed the original Ferguson classifications of the fainter dwarf population hold. In the future we hope measure redshifts for these galaxies to confirm cluster membership to fainter limits.

The confirmed cluster members and non-members occupy two distinct regions on the surface brightness-magnitude plot. We have found that both confirmed and unconfirmed background galaxies lie along the same locus and have a higher surface brightness than cluster members of the same magnitude. For surface brightnesses fainter than $22 \text{ V mag arcsec}^{-2}$ the two relations merge and distinguishing between members and non-members requires additional radial velocity measurements in order to make judgements of cluster membership.

The main limitation in the interpretation of the results is the resolution of the data. Our peak surface brightness measurements are largely influenced by resolution and seeing. The relation for background galaxies is simply a manifestation of this effect. Seeing acts in such a way that the measured peak surface brightness will always be fainter than the real central surface brightness. As background galaxies are less well resolved than cluster galaxies the seeing will have the dramatic effect of suppressing the central surface brightness. In particular background galaxies containing small cores, such as ellipticals and small scale-size dwarfs will be seriously affected by this method. With higher resolution observations and better seeing the separation between cluster and background galaxies would be more obvious down to much fainter surface brightness limits.

7.2 Surface brightness-magnitude relation

Our surface brightness-magnitude relation for Fornax Cluster members is consistent with previous studies (Phillipps et al. 1987; Caldwell & Bothun 1987). The E and dE galaxies follow a well defined sequence with increasing surface brightness corresponding to an increase in galaxy luminosity.

For our large sample of dwarf galaxies the observations are consistent with the recently published results of Deady et al. (2002) who investigated surface-brightness magnitude relation for 24 Fornax Cluster dwarfs. Total magnitudes were determined using the same methods as the photometry we have presented in this paper. However ex-

trapolated central surface brightnesses were obtained after fitting the galaxies with Sersic profiles.

The canonical surface brightness relation of Ferguson & Binggeli (1994) shows a clear break between the two populations. In that study the dE galaxies were plotted using photometric data from a complete sample of ≈ 200 early type galaxies in the Virgo cluster where the ‘mean’ central surface brightness was obtained using King models (Binggeli & Cameron 1991). The E galaxies and bulges were data obtained by Kormendy (1985) and included as many galaxies as possible which were near enough to have their cores resolved. Their results show that dwarf galaxies occupy a region of the plot with absolute magnitude limits of $-16 < M_B < -8$, the relationship indicating an increasing mean surface brightness with increasing luminosity. A break between the E and dE populations was identified.

Our model independent results are consistent with this observation. This break is clearly seen in the B band relation at a surface brightness of $21 \text{ B mag arcsec}^{-2}$ and becomes progressively weaker as you go to longer wavelengths. A discontinuity in surface brightness at $\sim 21 \text{ B mag arcsec}^{-2}$ is not entirely unexpected since it is known to be a transition point where many other properties within the E family are changing (Jerjen & Binggeli 1997).

In the canonical surface brightness relation the relationship for E galaxies is somewhat different to the dE population, the mean surface brightness increasing with decreasing luminosity. The interpretation of this segregation was concluded to result from the disparity of the model profiles fitted to each morphological type (Binggeli & Cameron 1991). Our model independent surface-brightness relation for E galaxies opposes this trend of increasing surface brightness with increasing luminosity. Our relation for E galaxies is similar to the results of Jerjen & Binggeli (1997), who also find that the population of dE and E galaxies smoothly and continuously merge. Their analysis was based on fitting Sersic profiles to the overall shape of galaxies, ignoring the innermost 3” ($\sim 300\text{pc}$) of the profiles. Their extrapolated surface brightnesses were systematically higher than the central surface brightnesses observed by Kormendy (1985) resulting in a shift that resolves the E-dE dichotomy. From this analysis it was concluded that the dichotomy was not evident because the cores of the E galaxies were not resolved.

A more recent analysis by Graham & Guzman (2003) show that the alleged dichotomy between E and dE galaxies can be resolved using Sersic profiles and when necessary a central point-source or PSF-convolved Gaussian. The relation for E galaxies depends on the ability to resolve the cores of the brightest elliptical galaxies. The dE galaxies are shown to display a continuous sequence with the brighter E galaxies such that the central surface brightness increases with increasing magnitude until core formation causes the most luminous E galaxies to deviate from the relation (Graham & Guzman 2003). Since our data is limited by resolution ($2.025'' \text{ pix} \approx 200\text{pc}$) we do not observe the relation for the most luminous E of increasing surface brightness with decreasing luminosity.

To test this hypothesis we have obtained high-resolution multicolour imaging of the cluster using the CTIO 4m Blanco Mosaic telescope. The image resolution ($0.27'' \text{ pix} \approx 25\text{pc}$) is such that we will be able to resolve the cores of

the E galaxies and see the trend of increasing surface brightness with increasing luminosity.

7.3 Dwarf Galaxies and the origin of the UCDs

It is not surprising that we find a spread of colours for the dwarf population since their low binding energies mean they are very susceptible to the cluster environment and can therefore display a wide range of evolutionary histories, even within the same subclass (Grebel 2001). Using integrated galaxy colours to investigate dwarf galaxy evolution is problematic. Galaxy colours result from many factors including galaxy metallicity, dust content and star-formation histories. For their sample of ten Fornax dE,Ns Held & Mould (1994) found a range of metallicities similar to those of intermediate ($[\text{Fe}/\text{H}] \sim -1.4 \text{ dex}$) to metal rich ($[\text{Fe}/\text{H}] \sim -0.7 \text{ dex}$) globular clusters. These metallicities are well correlated with the colours of Caldwell & Bothun (1987) which are consistent with the colours from our analysis.

Our photometry of the ultra-compact dwarfs exemplifies the problem of determining the membership status of high surface brightness objects. These objects were previously classified as foreground stars. Their isolated location on the surface brightness-magnitude plot seems to indicate they form a distinct class of objects.

From our results it is likely that we are observing remnant nuclei of a small sample of nucleated dwarf ellipticals which have been tidally stripped through their interaction with the central cD galaxy NGC 1399. This “galaxy threshing” is supported by simulations (Bekki et al. 2001) of infalling nucleated dwarf elliptical galaxies, which are tidally stripped as they orbit a central cD galaxy. The compact nucleus is weakly influenced by tidal forces. Since the contribution of light from the nuclei is typically 2% for nucleated dwarfs (Binggeli & Cameron 1991), the central surface brightness remains the same as the galaxy halo is stripped, however the apparent magnitude increases. On a surface brightness-magnitude plot this “stripping” manifests as a shift off the locus of the dE population towards a much fainter apparent magnitude. A further test for this theory would be to search the cores of clusters such as Virgo and Coma where similar objects may have been previously overlooked. Their location on the cluster surface brightness relation and colours would provide additional selection information.

It has also been suggested that one or more of the UCDs may form part of the bright end of the globular cluster population associated with NGC 1399 (Hilker et al. 1999; Mieske et al. 2002). Figure 8 is a colour-colour plot of the cluster dwarf population. The UCDs lie well within the cluster dwarf population and have similar colours to galactic globular clusters (Harris 1996). UCD5 lies away from the remaining population. As noted in section 4 we suspect higher resolution measurements will yield a similar V-I colour to the remaining population.

The errors of the photometry make an interpretation of the UCD colours by single burst stellar population models (i.e. Bruzual A. & Charlot (1993); Worthey (1994)) unreasonable. Again higher resolution observations will be required to make useful conclusions.

We are currently analysing deep multicolour imaging of the central 1 deg^2 region of the cluster, taken with the

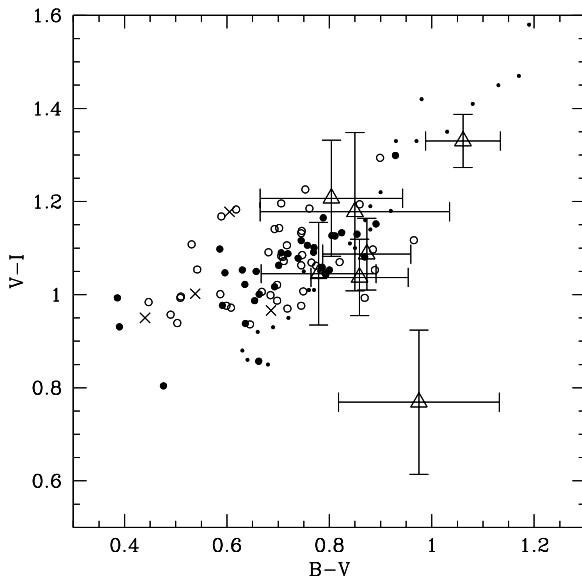


Figure 8. Colour-colour plot of the cluster dwarf population; dEs (small circles), dE_Ns from the FCC (filled circles), BCD/Im (small crosses) and UCDs (triangles) with error bars. Galactic globular clusters from the Harris catalogue (Harris 1996) are shown as small points.

CTIO 4m Blanco Mosaic telescope. The image resolution of the Mosaic data ($0.27''/\text{pixel}$) is such that the errors will be considerably less than the current photometry. Using the Sloan filter set ($u'g'r'i'z'$) we hope to accurately determine colours of the cores and halos of the dE,N population and the UCDs as well as the globular cluster population associated with NGC 1399. This will enable us to test the two main hypotheses for the origin of the UCDs and so we defer any further discussion of their colours until the presentation of the Mosaic data.

8 CONCLUSIONS

We have presented BVI photometry for a sample of 190 Fornax Cluster members. Our revised Fornax Cluster catalogue incorporates results from a number of recent spectroscopic surveys and also includes a small sample of recently discovered ultra-compact dwarf galaxies.

The UCDs have absolute magnitudes in the range $-13 < M_B < -11$. These results are consistent with previous R-band photometry of photographic images of the UCDs (Drinkwater et al. 2000) and B photographic colours of Deady et al. (2002). Although their colours $\langle V-I \rangle = 1.09$ and $\langle B-V \rangle = 0.89$ suggest an older stellar population not unlike globular clusters, they are much brighter than the most luminous of the globulars ($M_B \sim -11$) associated with NGC 1399 (Forbes et al. 1998). The UCDs lie off the surface-brightness magnitude correlation for dE galaxies which is consistent with the “galaxy-threshing” scenario by Bekki et al. (2001). This hypothesis is also supported by their location off the locus of the colour-magnitude relation for dE,Ns.

We have investigated the surface-brightness magnitude

relation for confirmed cluster members and background galaxies. Both populations occupy two distinct regions on the surface-brightness magnitude plot however at low luminosities the relations merge. This is due to the fact that the relation for background galaxies is largely influenced by the resolution and seeing of the observations.

For a more comprehensive analysis of the surface brightness-magnitude relation and the population of ultra-compact dwarfs we require much higher resolution observations. We are currently analysing deep multicolour imaging of the central 1° region of the cluster taken with the CTIO 4m Blanco telescope. The image resolution of $0.27''/\text{pixel}$ will provide us with more accurate surface brightness and colour measurements. Radial surface brightness profiles of the infalling dwarf population and the UCDs will further aid the investigation into the origin of the ultra-compact dwarfs. In addition, a comparison of the colours of cores and halos of infalling dE,N galaxies and the globular clusters associated NGC 1399 will enable us to further constrain the origin of the UCDs.

We also plan to investigate the population of infalling dwarf galaxies which lie outside our mosaic area, with particular emphasis on the merging Fornax sub-cluster. This will enable us to make a more detailed study of the colours of the Fornax population and the effect of the cluster environment on galaxy evolution.

9 ACKNOWLEDGEMENTS

We wish to thank Bryn Jones for helpful discussions on the photometry and suggestions regarding the analysis of our data. We are grateful to Mike Fall for suggesting the colour-magnitude analysis of the UCDs. We thank the referee M. Hilker for his very useful comments which improved the paper. We also thank our colleagues from the Fornax Cluster Spectroscopic Survey for providing the velocity data for our sample. This project was supported by grants from the Australian Research Council and the Australian Nuclear Science and Technology Organisation Access to Large Research Facilities scheme. This material is based in part upon work supported by the National Science Foundation under Grant No. 9970884 and carried out at the Institute of Geophysics and Planetary Physics, under the auspices of the U.S. Department of Energy by Lawrence Livermore National Laboratory under contract No. W-7405-Eng-48.

REFERENCES

- Bekki K., Couch W. J., Drinkwater M. J., 2001, ApJ, 552, L105
- Bertin E., Arnouts S., 1996, A&AS, 117, 393
- Binggeli B., Cameron L. M., 1991, A&A, 252, 27
- Bothun G. D., Impey C. D., Malin D. F., 1991, ApJ, 376, 404
- Bothun G. D., Impey C. D., Malin D. F., Mould J. R., 1987, ApJ, 94, 23
- Bruzual A. G., Charlot S., 1993, ApJ, 405, 538
- Caldwell N., Bothun G. D., 1987, ApJ, 94, 1126

Deady J. H., Boyce P. J., Phillipps S., Drinkwater M. J., 2002, "The Fornax Cluster Spectroscopic Survey: A Complete Sample of Cluster Dwarfs", astro-ph/0206510

Dirsch B., Richtler T., Geisler D., Forte J. C., Bassino L. P., Gieren W. P., 2003, *ApJ*, 125, 1908

Drinkwater M. J., Gregg M. D., Colless M., 2001, *ApJ*, 548, L139

Drinkwater M. J., Gregg M. D., Holman B. A., Brown M. J., 2001, *MNRAS*, 326, 1076

Drinkwater M. J., Jones J. B., Gregg M. D., Phillipps S., 2000, *Proc. Astron. Soc. Aust.*, 17, 227

Drinkwater M. J., Phillipps S., Gregg M. D., Parker Q. A., Smith R. M., Davies J. B., Jones J. B., Sadler E. M., 1999, *ApJ*, 511, L97

Drinkwater M. J., Phillipps S., Jones J. B., Gregg M. D., Deady J. H., Davies J. I., Parker Q. A., Sadler E. M., Smith R. M., 2000, *A&A*, 355, 900

Evans R., Davies J. I., Phillipps S., 1990, *MNRAS*, 245, 164

Ferguson H. C., 1989, *AJ*, 98, 367

Ferguson H. C., Binggeli B., 1994, *A&AR*, 6, 67

Ferguson H. C., Sandage A., 1988, *ApJ*, 96, 1520

Forbes D. A., Grillmair C. J., Williger G. M., Elson R. A. W., Brodie J. P., 1998, *MNRAS*, 293, 325

Graham A., Guzman R., 2003, *ApJ*, (in press, astro-ph/0303391)

Grebel E. K., 2001, in Dwarf galaxies and their environment 'Dwarf Galaxies in the Local Group and in the Local Volume (Invited Talk)". p. 45

Griersmith D., 1982, *ApJ*, 87, 462

Harris W. E., 1996, *ApJ*, 112, 1487

Held E. V., Mould J. R., 1994, *ApJ*, 107, 1307

Hilker M., Infante L., Vieira G., Kissler-Patig M., Richtler T., 1999, *A&AS*, 134, 75

Hilker M., Kissler-Patig M., Richtler T., Infante L., Quintana H., 1999, *A&AS*, 134, 59

Hilker M., Mieske S., Infante L., 2001, in Astronomische Gesellschaft Meeting Abstracts Vol. 18, "The Discovery of the Faintest Dwarfs in Nearby Galaxy Clusters". p. 520

Hilker M., Mieske S., Infante L., 2003, *A&A*, 397, L9

Impey C., Bothun G., Malin D., 1988, *ApJ*, 330, 634

Jerjen H., Binggeli B., 1997, in ASP Conf. Ser. 116: The Nature of Elliptical Galaxies; 2nd Stromlo Symposium "Are "Dwarf" Ellipticals Genuine Ellipticals?". p. 239

Kissler-Patig M., Kohle S., Hilker M., Richtler T., Infante L., Quintana H., 1997, *A&A*, 319, 470

Kormendy J., 1985, *ApJ*, 292, L9

Landolt A. U., 1992, *ApJ*, 104, 340

Mieske S., Hilker M., Infante 2002, *A&A*, 383, 823

Phillipps S., Davies J. I., Disney M. J., 1988, *MNRAS*, 233, 485

Phillipps S., Disney M. J., Kibblewhite E. J., Cawson M. G. M., 1987, *MNRAS*, 229, 505

Phillipps S., Drinkwater M. J., Gregg M. D., Jones J. B., 2001, *ApJ*, 560, 201

Sandage A., Binggeli B., 1984, *AJ*, 89, 919

Schlegel D. J., Finkbeiner D. P., Davis M., 1998, *ApJ*, 500, 525

Terlevich A. I., Caldwell N., Bower R. G., 2001, *MNRAS*, 326

Vazdekis A., Kuntschner H., Davies R. L., Arimoto N., Nakamura O., Peletier R., 2001, *ApJ*, 551, L127

Visvanathan N., Sandage A., 1977, *ApJ*, 216, 214

Worthey G., 1994, *ApJS*, 95, 107